J Biomol NMR (2011) 51:357–367
DOI 10.1007/s10858-011-9563-8

ARTICLE

The use of ^{1}H–^{31}P GHMBC and covariance NMR to unambiguously determine phosphate ester linkages in complex polysaccharide mixtures

Edward R. Zartler · Gary E. Martin

Received: 8 July 2011 / Accepted: 25 August 2011 / Published online: 16 September 2011

Abstract Poly- and oligo-saccharides are commonly employed as antigens in many vaccines. These antigens contain phosphoester structural elements that are crucial to the antigenicity, and hence the effectiveness of the vaccine. Nuclear Magnetic Resonance (NMR) is a powerful tool for the site-specific identification of phosphoesters in saccharides. We describe here two advances in the characterization of phosphoesters in saccharides: (1) the use of ^{1}H–^{31}P GHMBC to determine the site-specific identity of phosphoester moieties in heterogeneous mixtures and (2) the use of Unsymmetrical/Generalized Indirect Covariance (U/GIC) to calculate a carbon-phosphorus 2D spectrum. The sensitivity of the ^{1}H–^{31}P GHMBC is far greater than the "standard" ^{1}H–^{31}P GHSQC and allows long-range $^{3-5}J_{HP}$ couplings to be readily detected. This is the first example to be reported of using U/GIC to calculate a carbon-phosphorus spectrum. The U/GIC processing affords, in many cases, a fivefold to tenfold or greater increase in signal-to-noise ratios in the calculated spectrum. When coupled with the high sensitivity of ^{1}H–^{31}P HMBC, U/GIC processing allows the complete and unambiguous assignments of phosphoester moieties present in heterogeneous samples at levels of ~5% (or less) of the total sample, expanding the breadth of samples that NMR can be used to analyze. This new analytical technique is generally applicable to any NMR-observable phosphoester.

Keywords Phosphorus · Unsymmetrical indirect covariance · Generalized indirect covariance · Multiple bond coupling · Carbon-phosphorus spectrum

Abbreviations

αRha	L-α-Rhamnose
βGlc	β-D-Glucose
β-ManNAc	β-2-Acetamido-mannose
β-GlcNAc	β-2-Acetamido-glucose
α-GlcNAc	α-2-Acetamido-glucose
NMR	Nuclear magnetic resonance spectroscopy
GHMBC	Gradient heteronuclear multiple bond correlation
GHMQC	Gradient heteronuclear multiple quantum correlation
GHSQC	Gradient heteronuclear single quantum correlation
PC	Phosphocholine
U/GIC	Unsymmetrical/generalized indirect covariance
MS	Mass spectrometry

Introduction

Phosphodiesters play a central role in biology (Watson and Crick 1953). Phosphodiesters are structural components in molecules like nucleic acids and bacterial cell wells, regulatory switches, and play a crucial role in the inflammatory response (John et al. 2009a, b). NMR has been used to characterize phosphates in many of these systems. In these

Electronic supplementary material The online version of this article (doi:10.1007/s10858-011-9563-8) contains supplementary material, which is available to authorized users.

E. R. Zartler (✉)
Vaccine Analytical Development, Merck Research Labs, Merck & Co., West Point, PA 19486, USA
e-mail: teddyzartler@gmail.com

G. E. Martin
Structure Elucidation Group, Merck Research Labs, Merck & Co., Summit, NJ 07901, USA

cases, NMR is used to identify the proton-phosphorus linkages (via $^{3}J_{HP}$ couplings) of the molecule of interest. Minor components, such as substoichiometric species, contaminants, etc., are typically not detected, or have been ignored, in these studies. NMR can also be used to follow enzymatic reactions where phosphates are a reaction component (Marino 2011). However, these studies focused on changes in the chemical shift environment of the phosphate and not on the structural aspect, i.e. site-specific monitoring of the phosphate. Structural studies of the product of phosphate-containing enzymatic reactions also are reported, but in these cases, the product was studied in isolation and not as a mixture. Many vaccines contain components that incorporate phosphoester moieties, such as capsular polysaccharides (bCW) or lipooligosaccharides (LOS) as antigens (Abeygunawardana et al. 2000; Aubin et al. 2010). Bacterial poly- and oligo-saccharides often contain structural phosphates and quite frequently non-structural, pendant phospho-polyalcohols. Mass spectrometry (MS) is a powerful tool for the detection of phosphorylation. However, in samples where there can be multiple sites of attachment (as in phospho-saccharides), it is extremely challenging to employ MS to determine site-specific information, although it is not impossible. It is possible that heterogeneity in these pendant phospho-polyalcohols could affect immunogenicity of bacterial poly- and oligo-saccharides, offering an additional "escape" route, akin to variations in O-acetylation (Zartler et al. 2009). NMR has been the method of choice for obtaining this information from poly- and oligo-saccharides due to its facile ability to obtain site-specific connectivity information. With this as our goal, we investigated novel techniques to further characterize our vaccines.

The classical way of obtaining information on ^{1}H–^{31}P linkages is through analysis of ^{1}H couplings in a 1D ^{31}P spectrum (Williamson and Griffin 1968), which could be acquired with room temperature broadband probes. The advent of inverse detection probes with a coil tuned for ^{31}P led to the development of the ^{1}H–^{31}P HMQC and ^{1}H–^{31}P HSQC experiments for the detection of ^{1}H–^{31}P connectivities. These experiments have a long history of utility (Lindon et al. 1986; Chary et al. 1993; Luy and Marino 2001; Kozminski et al. 2003; Catoire 2004); however, they are limited to detection of $^{3}J_{HP}$ correlations, really H–C–O–P couplings. The majority of the pulse sequence development for ^{31}P has focused on applications in nucleic acid characterization. These experiments are typically variations on the 3D ^{1}H–^{13}C–^{31}P experiment (e.g. Malon and Koshino 2007), although 2D variants exist for many of them. Another drawback of these methods is that many of them are designed to be used with ^{13}C-labeled molecules; something that is simply not available in a product development environment. It is also required to fully characterize a product in clinical development (ICH Harmonised Tripartite Guideline: Q6B). In a product development environment the assays used to characterize the product must be robust and able to evaluate the product as it is made, i.e. without labeling.

Recent development efforts in ^{1}H–^{31}P spectroscopy have focused on the structural characterization of small phosphate-containing molecules, typically metabolites or enzymatic products (Majumdar et al. 2009, 2010). The ^{1}H–^{31}P–^{31}P-COSY experiment described by Majumdar and co-workers suffers from the need to adjust the delays within the sequence to match the specific phosphorus signal in a pyrophosphate moiety to be observed. Majumdar and co-workers describe a process for determining the appropriate J_{PP}, but this process is highly empirical and needs to be performed for every system. Choosing the wrong coupling constant can lead to almost complete loss of signal. However, despite this limitation, the method is highly sensitive and able to pick up multiple phosphorus signals with the choice of appropriate experimental parameters. 2D H–X (X = ^{31}P) COSY and 2D HCP can also be used to determine H–P connectivities.

The H–X HMBC pulse sequence was originally proposed to detect multiple bond heteronuclear connectivities using proton detection (Bax and Summers 1986). This experiment was initially used with X = ^{13}C and is a variation of the HMQC experiment with several notable changes: the defocusing period is typically optimized for $1/(2*^{n}J_{XH})$ [5–10 Hz for ^{13}C], the refocusing period is omitted, and ^{1}H acquisition is performed without X-nucleus decoupling. The H–X HMBC experiment also can utilize gradients for coherence selection, resulting in higher quality spectra, and low-pass filters to minimize direct responses. The H–X HMBC experiment is typically run with X = ^{13}C (Martin 2002a, b) or ^{15}N (Marek et al. 2002, 2007; Martin and Hadden 2000; Martin 2005; Martin and Williams 2010). ^{1}H–^{31}P HMBC has a limited history in determining phosphate linkages in small molecules. Keniry (1996) reported the use of ^{1}H–^{31}P HMBC to determine the phosphodiesters in a 10-mer DNA duplex using a gradient-selected experiment. Davies and co-workers (Davies et al. 2000; Veselkov et al. 2001) used a non-gradient ^{1}H–^{31}P HMBC to identify the linkages in short DNA tetramers and subsequently used it to monitor changes in the backbone as a function of drug binding. Subsequent reports of ^{1}H–^{31}P HMBC applications have focused almost solely on its use to estimate ^{1}H–^{31}P couplings in small molecules (Willker and Leibfritz 1995; Kozminski et al. 2003; Sakamoto et al. 2006). To the best of our knowledge, there have been no reports of ^{1}H–^{31}P HMBC on biological samples. Previous ^{1}H–^{31}P HMBC studies were limited by the equipment of the time, typically a 500 MHz spectrometer equipped with

a non-cryogenic broadband or proton observe probes. Technological advances in the interceding years have led to great improvements in the quality of NMR spectra. Specifically, the development of cryogenic probes (Martin 2002a, 2005; Martin and Williams 2005) has led to a significant increase in detected signal. We capitalize on these improvements in signal to noise (S/N) to use the $^{1}H–^{31}P$ HMBC and $^{1}H–^{13}C$ HSQC to assign resonances in minor populations (<5%) in heterogeneous samples.

Polysaccharide literature has numerous examples of disagreement upon specific locations for phosphomoieties. In ST23F polysaccharide (a component of the vaccines Pneumovax®, Prevnar-13®, and Synflorix®), there are conflicting reports of the site of the phospho-glycerol (Roy and Roy 1984; Jones 1985; Richards and Perry 1988). In this case, these assignments were inferred based upon ^{31}P couplings observed in the ^{1}H spectrum, i.e. without direct detection of proton-phosphorus linkages. The $^{1}H–^{31}P$ GHMBC experiment can directly determine these linkages instead of relying on inferred structure (Zartler, unpublished results). Problems like these arise due to the severe overlap in both the ^{1}H and ^{13}C dimensions of saccharide ring protons. Typically in polysaccharides the majority of proton resonances fall within a one ppm range (~3–4 ppm). Consequently, spectral overlap can limit the ability to unambiguously identify the phosphate-substituted position. Additionally, there is a growing body of evidence in the lipooligosaccharide (LOS) literature that LOS can be heterogeneously phosphorylated with phosphate, pyrophosphate, phosphoethanolamine, pyrophosphoethanolamine, etc. (John et al. 2009a, b). Heterogeneity and variability between different strains taxes the capability of current methods to detect and characterize these minor components. These minor components are also known to play a major role in immunogenicity of the molecule, which can have adverse affects on vaccines composed of these molecules. Thus, it is imperative to develop a robust method that can characterize these minor populations.

The capsular polysaccharide of *Streptococcus pneumoniae* serotype 19F (ST19F) is a component of the pneumococcal vaccines Pneumovax®, Prevnar-13®, and Synflorix®. This polysaccharide has been well characterized by NMR (Abeygunawardana et al. 2000; Kamerling 2000; Pujar et al. 2004; Xu et al. 2005), and unlike ST23F, there are no ambiguities concerning its structure. ST19F polysaccharide (PS) is a polymer composed of a linear repeat of [-4-D-α-Gluose-1-L-α-Rhamnose-phosphate-4-D-β-2-acetamido-mannose-1-] (Fig. 1a). Capsular polysaccharide preparations are typically contaminated by teichoic acid (also known as c-polysaccharide, c-PS), at anywhere from 0 to 20 mol percent (Xu et al. 2005). The c-PS structure from *S. pneumoniae* is relatively consistent from strain to strain, although differences do exist (Draing et al. 2006). The c-PS associated with ST19F PS is a linear repeat of [-3-α-2-acetamido-4-amino-2,4,6-trideoxy-galactose-1-4-α-D-(2-acetamido)-galactose(6-phosphocholine)-

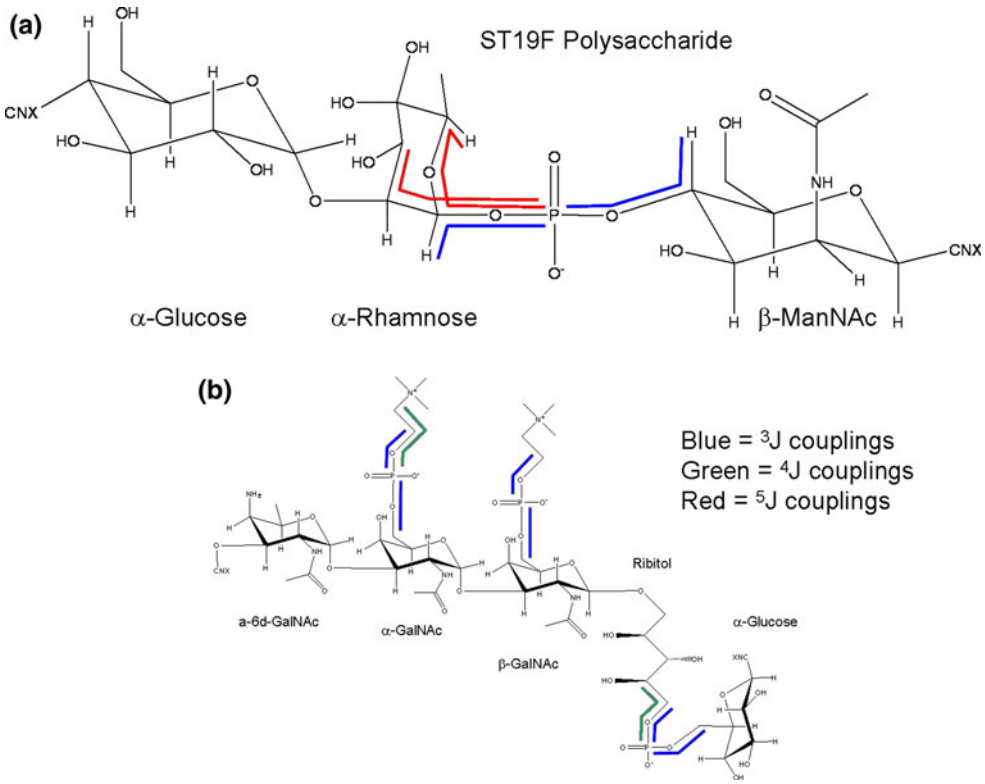

Fig. 1 Structures of ST19F (**a**) and c-PS (**b**). The *blue lines* indicate ^{3}J couplings, *green lines* ^{4}J couplings, and *red lines* ^{5}J couplings that are detected in the $^{1}H–^{31}P$ GHMBC spectra

1-3-β-D-(2-acetamido)-galactose(6-phosphocholine)-1-1-ribitol-5-phosphate-6-β-D-glucose-1-] (Fig. 1b). Of particular note for this study is the presence of one phosphodiester in ST19F and three in c-PS.

^{1}H–^{13}C HMBC is commonly used to detect 2–4 bond long-range correlations, $^{2-4}J_{CH}$ (Martin 2002a, b; Schoeberger et al. 2011). In most cases, $^{2}J_{CH}$ correlations are not observed. These correlations ($^{2-4}J_{CH}$) are based upon proton-carbon couplings (and obey the Karplus equation) and for many common cases (where the coupling is small) magnetization is not transferred and the coherence is not observed. A wide range of ^{1}H–^{13}C experiments have been developed to address problems in observing small, long-range heteronuclear correlations (Martin 2002a, b).

We present here the use of the ^{1}H–^{31}P HMBC experiment to identify phosphoesters in polysaccharides. In this report we demonstrate the following: (1) ^{1}H–^{31}P HMBC is a highly sensitive experiment for detecting ^{1}H–^{31}P linkages; (2) $^{3-5}J_{HP}$ couplings can be detected; and (3) Unsymmetrical and Generalized Indirect Covariance (U/GIC) can be used to calculate the carbon-phosphorus 2D spectrum to circumvent some of the problems inherent to oligosaccharide proton resonance overlaps. This is the first example of using U/GIC calculations to produce a carbon-phosphorus spectrum.

Materials and methods

NMR spectroscopy

All data were acquired on a Bruker Avance three channel spectrometer operating at 700 MHz and equipped with a cryogenically-cooled TCIP ^{1}H/^{13}C/^{31}P probe. All data were acquired at 49°C. Data were processed either using Mnova (Mestrec.com) or ACD Spectrus 2011. ST19F was ~5 mg/ml in D_2O containing DMSO-d_6 and DSS-d_6 as calibrant and reference standard, respectively (Isotec).

The ^{1}H–^{13}C GHMBC pulse sequence (hmbcgplpndqf) was used to set up the ^{1}H–^{31}P GHMBC experiments reported. This pulse sequence uses gradients for coherence selection, no decoupling during acquisition in magnitude mode, and incorporates a low-pass J-filter. The gradients were calculated by the au program 'gradratio' and were: gp1:gp2:gp3 60:20:72.4. Based upon the 1D ^{31}P spectrum (Supplemental Figure 1) the experiment was set up to afford a 12 ppm spectral width in the indirect dimension F_1 centered at 0 ppm. The $^{1}J_{HP}$ coupling for the low-pass filter was varied from 5 to 200 Hz and the $^{n}J_{HP}$ (the long-range coupling constant) was modulated from 2 to 200 Hz. A spectrum was acquired without the low-pass filter using $^{n}J_{HP} = 20$ Hz. Each spectrum was acquired with 32 scans as a 2,048 × 128 pt matrix with spectral widths of 7,002.8 and 3,401.3 Hz, respectively, affording a digital resolution of 3.4 and 26 Hz/pt. The ^{1}H–^{13}C GHSQC was acquired with 32 scans as a 2,048 × 256 pt matrix with spectral widths of 7,002.8 and 21,128.6 Hz, respectively, affording a digital resolution of 3.4 and 82.5 Hz/pt. The 1D ^{1}H spectrum was acquired with 16 scans and a sweep width of 7,002.8 Hz. Referencing was done relative to DSS-d_6 or DMSO-d_6 for ^{1}H and ^{13}C, and indirectly for ^{31}P.

Unsymmetrical/generalized indirect covariance

The ^{13}C–^{31}P 2D correlation spectrum was calculated using the GIC method of Snyder and Brüschweiler (2009) contained in the Spectrus 2011 program package from ACD. The square root of the resulting spectrum was taken to reduce spurious signals (Chen et al. 2007; Martin et al. 2011a, b; Snyder and Brüschweiler 2009). Care was taken to insure that the common frequency domain (^{1}H) employed identical transmitter locations and spectral widths in both the multiplicity-edited ^{1}H–^{13}C GHSQC and ^{1}H–^{31}P GHMBC spectra used in the calculation. Data were re-processed to 2 K × 2 K points prior to the covariance calculation.

Results

ST19F and c-PS assignments

Assignments of ST19F polysaccharide (ST19F) were adapted from Jennings et al. (1980) and confirmed by ^{1}H–^{1}H TOCSY, ^{1}H–^{1}H GCOSY, and ^{1}H–^{13}C GHSQC. One item to note is that based upon Jennings et al. (1980) the resonance for αGlc H1 should be at 5.00/100.6 and the βManNac is 4.86/98.90. Instead, the proper ^{13}C chemical shift for αGlc is 98.6 and for βManNac it is 100.2; these two ^{13}C assignments were switched. The assignments of c-PS were adapted from Draing et al. (2006). The resonances involved in phosphodiesters were confirmed by ^{1}H–^{1}H TOCSY, ^{1}H–^{1}H GCOSY, ^{1}H–^{13}C GHSQC, ^{1}H–^{13}C GHMBC, and ^{1}H–^{13}C GHSQC-TOCSY. A summary of assignments of both of these molecules can be found in the supplemental information (Supplemental Table 1).

^{1}H–^{31}P HMBC

Figure 2a shows the multiplicity-edited ^{1}H–^{13}C GHSQC of ST19F and reveals the very good chemical shift dispersion in both ^{1}H and ^{13}C dimensions. The two resonances involved in the phosphodiester of the backbone are indicated by arrows and labeled. The horizontal trace of Fig. 2a shows the 1D ^{1}H spectrum of ST19F, while the vertical trace shows the 1D ^{13}C spectrum. It is important to note

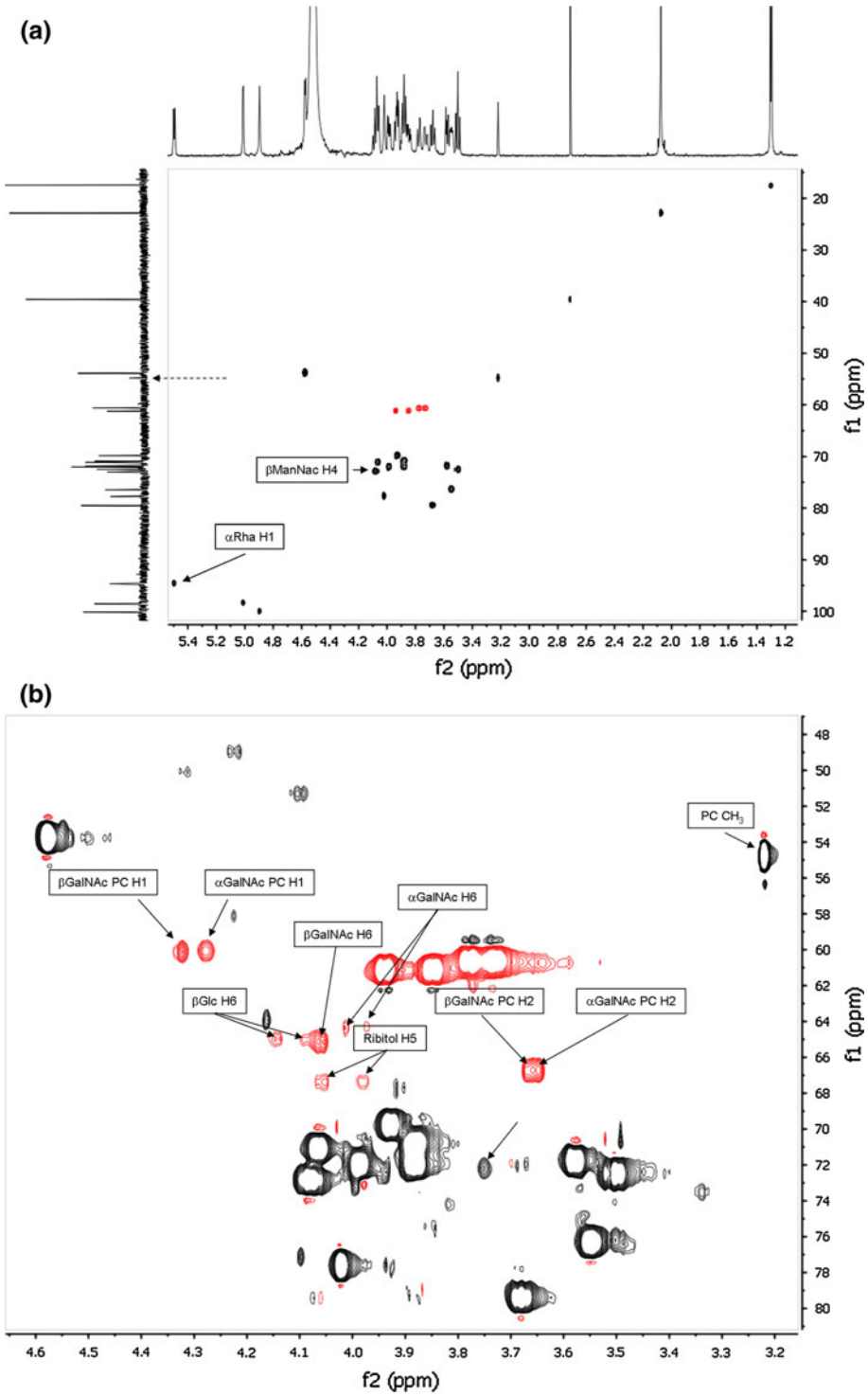

Fig. 2 **a** ^{1}H–^{13}C HSQC showing those peaks corresponding to the capsular polysaccharide of ST19F (~97% of sample mass). The *horizontal* and *vertical* axes show the ^{1}H and ^{13}C direct-observe spectra, respectively. The two ST19F PS resonances involved in the phosphodiester are labeled and indicated. The *arrow* pointing to the ^{13}C axis indicates the only observable c-PS carbon resonance. **b** ^{1}H–^{13}C HSQC with the threshold greatly reduced to show those peaks corresponding to the c-polysaccharide contaminating the sample (~3% of sample mass). Peaks involved in the c-PS phosphodiester are indicated and labeled. The sole peak denoted with an *arrow* but not labeled is discussed in the text

that the ^{13}C 1D spectrum has only one resonance from c-PS, indicated by the dashed arrow. The c-PS resonance is observed at 3.22/54.81 (Figs. 1b, 2a), which is due to the 6 methyls from phosphocholine. c-PS is present at ~3.0 mol percent (compared to capsular PS) (Abeygunawardana et al. 2000). Figure 2b shows the same spectrum zoomed on the ring proton region with the threshold reduced by ~tenfold. The resonances of c-PS involved in phosphodiesters are labeled. It is important to note that these resonances are largely well resolved in the ^{13}C dimension, but highly overlapped with capsular polysaccharide resonances in the ^{1}H dimension.

The ^{1}H–^{31}P HMBC spectrum with $^{n}J_{HP} = 200$ Hz (2.5 ms) is shown in Fig. 3a with four distinct ^{31}P chemical

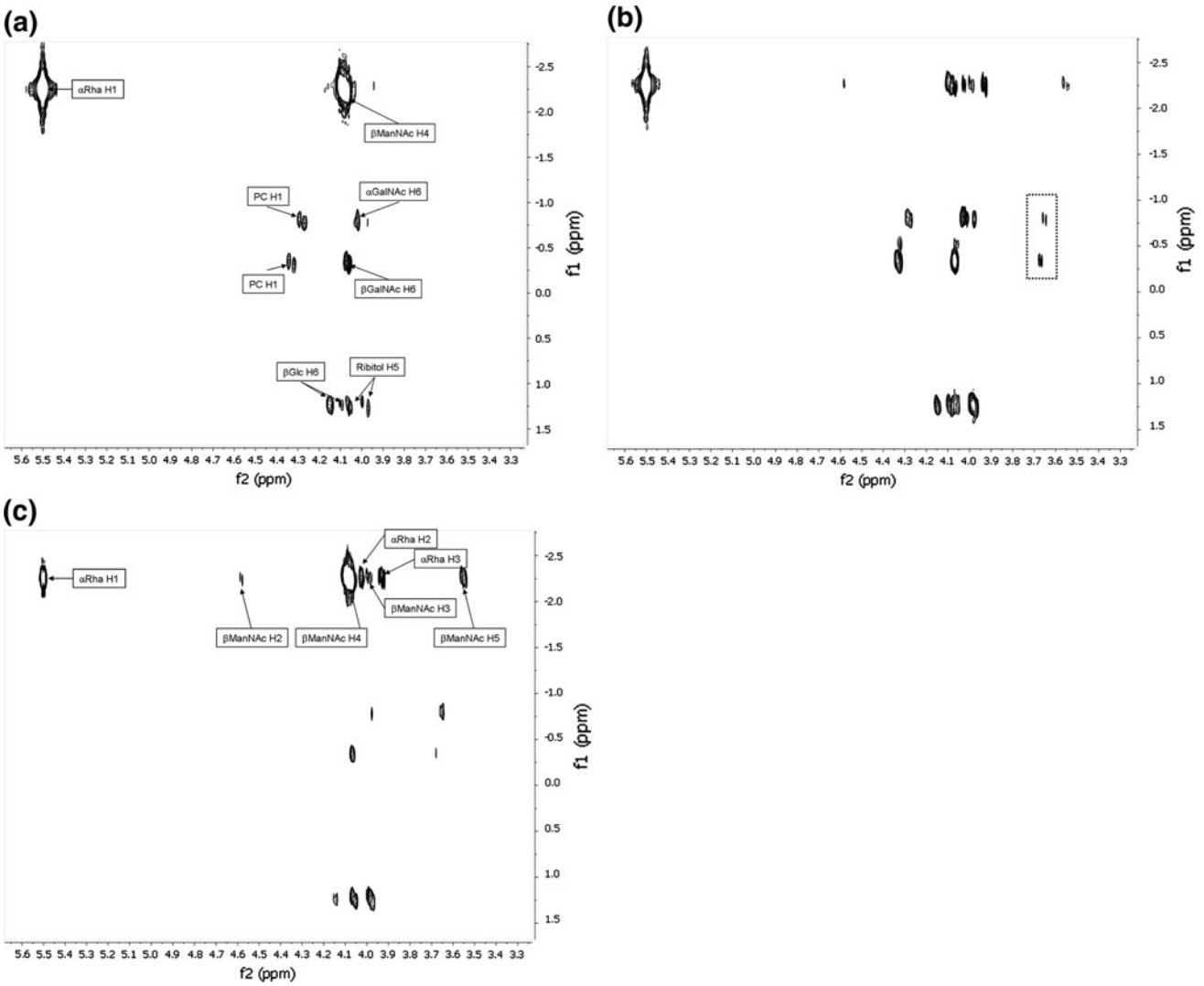

Fig. 3 ^{1}H–^{31}P HMBC Spectrum of ST19F. **a** $^{n}J_{HP} = 200$ Hz which detects short range couplings primarily. $^{3}J_{HP}$ assignments are given. **b** $^{n}J_{HP} = 5$ Hz showing a compromise that detects both short (^{3}J) and long range couplings ($>^{3}J$). The *dotted box* shows the $^{4}J_{HP}$ couplings that are now detected from the pendant phosphocholine in c-PS, c) $^{n}J_{HP} = 2$ Hz detecting preferentially long range ($>^{3}J$) couplings. $^{4,5}J_{HP}$ assignments are given

Table 1 ^{31}P chemical shifts

Component	ppm
ST19F polysaccharide	−2.27
c-PS αGalNAc-P-phosphocholine	−0.81
c-PS βGalNAc-P-phosphocholine	−0.33
βGlucose-P-ribitol	1.26

shifts (Table 1.) With this very short delay, the most prominent couplings observed are the $^{3}J_{HP}$ ("directly bound"), (Fig. 1a, b, blue lines). When the long-range delay was optimized as $^{n}J_{HP} = 5$ Hz (100 ms) (Fig. 3b) all of the $^{3}J_{HP}$ couplings observed with the short delay are again observed. The correlation observed at 4.08, −2.27 (^{1}H, ^{31}P ppm) (βManNAc H4) is reduced in intensity by over tenfold relative to the spectrum recorded with $^{n}J_{HP} = 200$ Hz (2.5 ms). The resonance at 5.50, −2.27 (αRha H1) is only reduced by ∼30%. The advantage of this shorter $^{n}J_{HP}$ is in the observance of additional couplings which correlate to $^{4,5}J_{HP}$, e.g. the correlations at 3.65, −0.81 and 3.67, −0.33 (Fig. 3b, dotted box) (Fig. 1a, b, green and red lines). Additional resonances arising from $^{4,5}J_{HP}$ are also seen at −2.26 ppm, corresponding to the ST19F PS. Specifically, correlations from the βManNAc H3, H2, and H5 and the αRha H2 and H3 are observed. Figure 3c shows the extreme example of $^{n}J_{HP} = 2$ Hz (250 ms). In this case, the $^{4,5}J_{HP}$ couplings have maximum intensity, while the $^{3}J_{HP}$ couplings are greatly reduced in intensity, or are totally absent. As expected for a through-

bond coupling, response intensities modulate as a function of the $^{n}J_{HP}$ (Supplemental Figure 2). The modulation is not purely sinusoidal most likely due to the ^{1}H–^{1}H couplings observed as "twisting" in the indirect dimension (see below). Unlike the ^{1}H–^{31}P HMBC spectrum, the ^{1}H–^{31}P HSQC experiment needs to have the '$^{1}J_{HP}$' (really $^{3}J_{HP}$) appropriately set. With an improper $^{3}J_{HP}$, important resonances can be completely missed. This is another advantage inherent to the ^{1}H–^{31}P HMBC sequence; the basic HMBC pulse sequence does not use a $^{1}J_{XH}$ coupling. However, when a low-pass J-filter is included, as in the sequence we used, this becomes a parameter to be investigated. In this system, we found that the $^{1}J_{HP}$ value did not play a major role in spectral quality, although it did have an effect on intensity (as would be expected). Little effort was spent in optimizing this parameter, but we found that $^{1}J_{HP} = 40$ Hz was a robust compromise value. When ^{1}H–^{31}P data were acquired without the low-pass filter there was no significant difference in the resulting spectrum when compared to the spectrum obtained with the low-pass filter. The only difference was an increase in ^{1}H–^{1}H couplings observed in the direct dimension, as would be expected.

Calculation of ^{13}C–^{31}P correlation spectra using covariance methods

Covariance NMR methods have recently been reviewed by Snyder and Brüschweiler (2010). While covariance NMR methods can take many forms, the variant germane to the present study involves the covariance co-processing of heteronuclear 2D NMR spectra that share a common frequency domain, originally defined as unsymmetrical indirect covariance (UIC) processing (Blinov et al. 2006a, b). More recently Snyder and Brüschweiler (2009) described a related method that they labeled generalized indirect covariance (GIC) processing. The covariance processing method does not create any new correlation information but rather sorts the correlation data contained in the two component spectra in a useful way (Fig. 4). Hence, the resonance overlap problems inherent to the proton

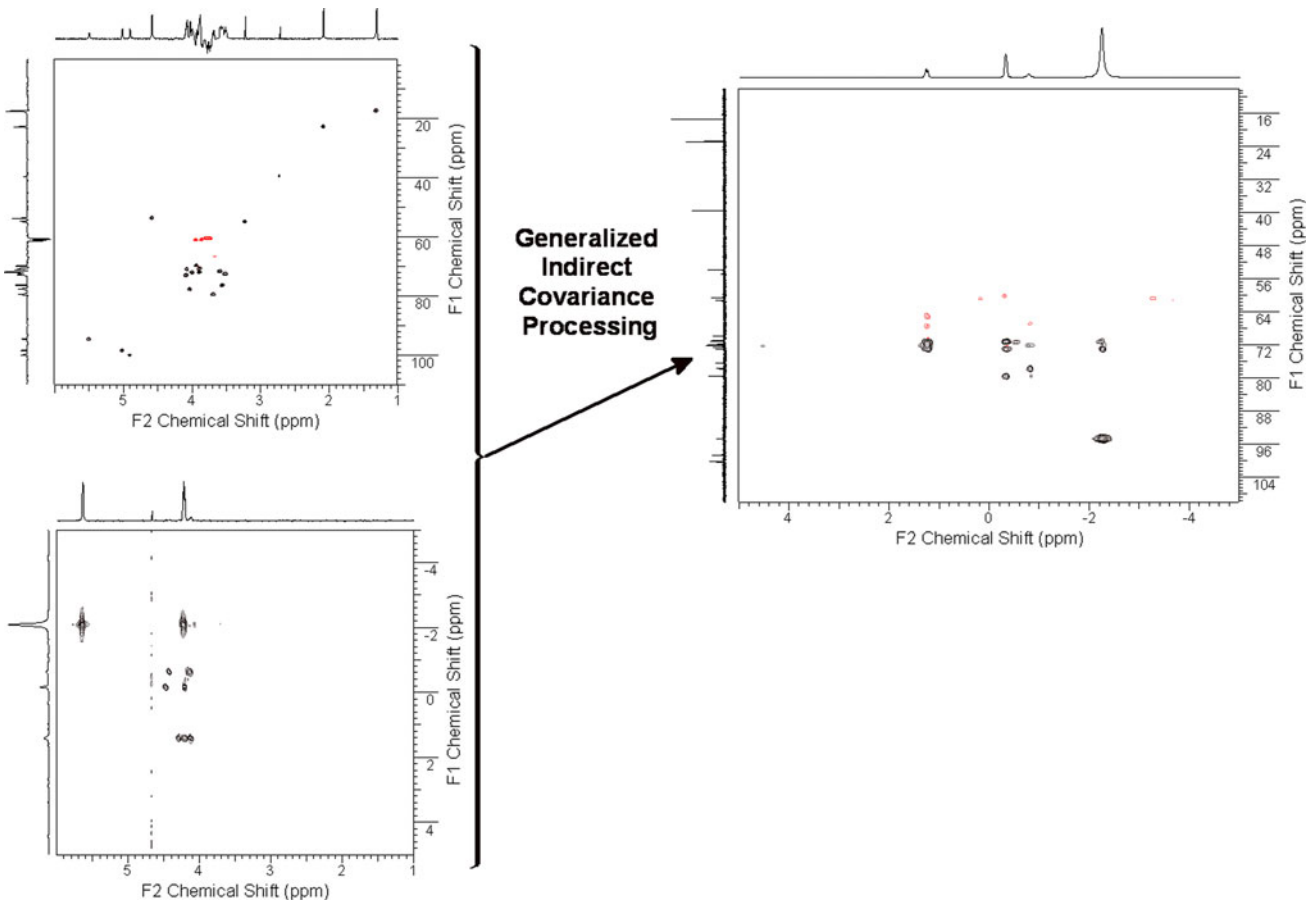

Fig. 4 The combination of the multiplicity-edited ^{1}H–^{13}C GHSQC and ^{1}H–^{31}P GHMBC yields a ^{13}C–^{31}P covariance spectrum. The multiplicity information from the ^{1}H–^{13}C GHSQC is retained

dimension of the ^{1}H–^{13}C GHSQC spectrum of an oligo- or polysaccharide can be circumvented by sorting the ^{1}H–^{31}P correlations from the GHMBC spectrum as a function of ^{13}C shifts in a ^{13}C–^{31}P long-range correlation spectrum. Thus, the multiplicity-edited ^{1}H–^{13}C GHSQC and ^{1}H–^{31}P GHMBC spectra were co-processed using the generalized indirect covariance (GIC) method of Snyder and Brüschweiler (2009) affording the first example of a ^{13}C–^{3}P long-range correlation spectrum shown in Fig. 5. Previous work has demonstrated the viability of this approach through the correlation of ^{13}C–^{15}N correlation spectra from multiplicity-edited ^{1}H–^{13}C GHSQC and ^{1}H–^{15}N GHMBC spectra (Martin et al. 2007a, b).

Usefully, UIC/GIC calculations that combine a low-sensitivity experiment, e.g. 1,1-ADEQUATE, with a high-sensitivity experiment, such as a multiplicity-edited ^{1}H–^{13}C GHSQC, can result in a five- to as much as a 20-fold enhancement in the correlations from the low-sensitivity experiment. (Martin et al. 2011a, b). Detecting the low sensitivity correlations with the apparent sensitivity of the high sensitivity experiment through covariance processing allows the low-sensitivity data to be acquired much more rapidly or conversely with less sample. In the case of a sample containing a low level component, for example the 3% c-PS component of the ST19F sample, the enhanced sensitivity derived from covariance processing allows correlations for the minor component of the sample to be examined with much greater facility.

Discussion

^{1}H–^{31}P HMBC

We have demonstrated the utility of ^{1}H–^{31}P HMBC for characterizing phosphodiesters of polysaccharides. Of particular note, the ^{1}H–^{31}P HMBC experiment is sufficiently sensitive that all proton-phosphorus linkages of a component present at 3% of the sample can be readily detected. The experiment is also highly "tuneable." By the appropriate choice of the long-range coupling constant ($^{n}J_{HP} > 100$ Hz) $^{3}J_{HP}$ linkages can be preferentially detected, or $^{3-5}J_{HP}$ ($^{n}J_{HP} < 50$ Hz) linkages can be detected in a single spectrum. The highly modulated nature of the $^{n}J_{HP}$ indicates that this is not a through-space coupling. The use of the low-pass J-filter in the sequence only affects the spectra in a qualitative sense. The '$^{1}J_{HP}$' value used in the low-pass J-filter is relatively insensitive, but we have empirically determined that a good value is 40 Hz. The ^{1}H–^{31}P HMBC can also be used for monoesters or detecting pyrophosphoesters (Data Not Shown).

As seen in Fig. 3a, there is "twist" in the indirect dimension in some of the crosspeaks in the ^{1}H–^{31}P HMBC spectrum, notably at 4.32, −0.32 and 4.27, −0.83. These can be attributed to ^{1}H–^{1}H couplings (Claridge and Perez-Victoria 2003). The use of a sequence containing a constant-time (CT) element would reduce or eliminate these couplings. However, since ^{1}H–^{31}P HMBC spectra are not crowded in the proton or phosphorus dimension,

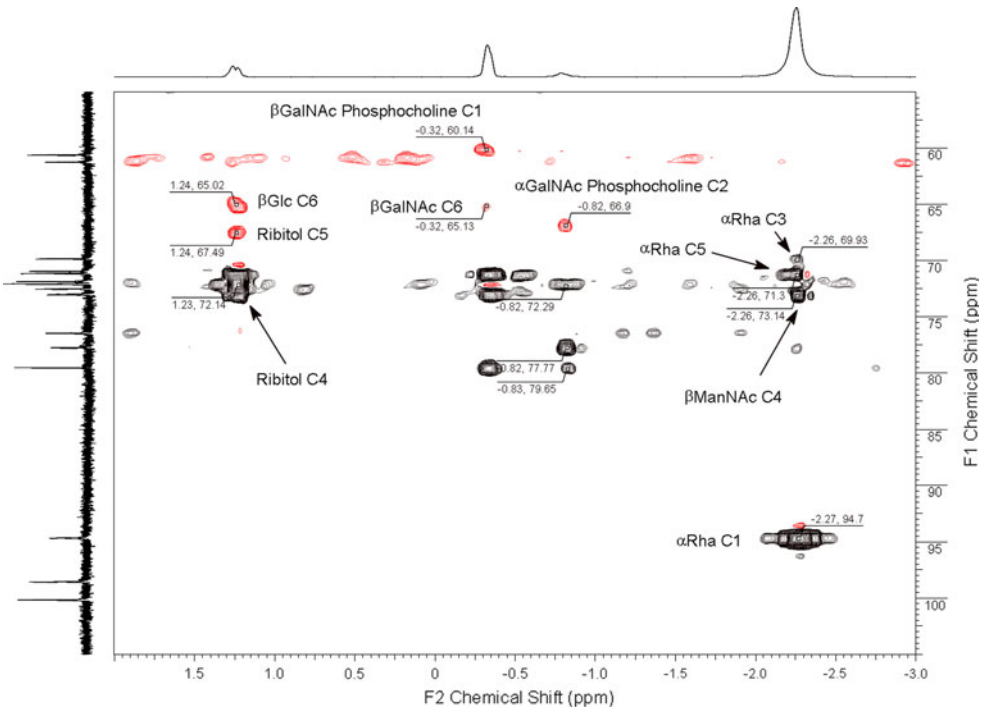

Fig. 5 Expansion of the ^{31}P–^{13}C covariance spectrum. Assignments of phosphodiester from polysaccharide ($\delta P = -2.27$ ppm) and the three phosphodiesters from c-polysaccharide ($\delta P = 1.26$, -0.34, and -0.81 ppm). Unambiguous assignments from this calculated spectrum are labeled

twisting does not create any assignment ambiguities. For systems where there is a wide ^{31}P spectral width required, a band selective experiment like the IMPACT-HMBC would be very useful (Furrer 2010). A further advantage of the ^{1}H–^{31}P HMBC method is that it does not require any specific knowledge of $^{3}J_{HP}$ coupling constants. Other ^{1}H–^{31}P detection methods require a good estimate of this coupling or empirical optimization to obtain maximum intensity. The HMBC sequence only requires the choice of $^{n}J_{HP}$. This coupling can be used robustly for "compromise" spectra (e.g. 10–40 Hz), or tuned to detect preferentially short range (100–200 Hz) or long-range (<5 Hz) couplings.

One major advantage of ^{1}H–^{31}P HMBC data compared to ^{1}H–^{31}P HSQC data is that multiple ^{1}H resonances can be correlated to the phosphorus resonance. Multiple correlations to each ^{31}P resonance aids in the assignment of sites of connectivity by giving additional resonances to use as "anchor points". For example, in polysaccharides, where ^{1}H resonances can be highly overlapped, having multiple peaks with which to make an assignment increases the confidence of the assignment. When these long-range ^{1}H–^{31}P correlations are ambiguous, then ^{13}C–^{31}P correlations can be used to resolve these ambiguities. As discussed below, we have taken a mathematical, rather than spectroscopic, approach to produce these correlations.

Covariance discussion

We show here the first example of covariance co-processing to calculate a ^{13}C–^{31}P heteronuclear long-range correlation spectrum. While there are some examples of ^{13}C–^{31}P heteronuclear shift correlation found in the literature, there are no contemporary examples of such spectra (Sims et al. 1989; Berger 2010). Covariance methods offer the means of mathematically combining 2D NMR spectra that share a common frequency domain, e.g. the multiplicity-edited ^{1}H–^{13}C GHSQC and ^{1}H–^{31}P GHMBC experiments used in the present example. Using covariance co-processing also allows the mathematical combination of high sensitivity experiments that can be advantageous relative to the acquisition of, for example, a ^{31}P-detected ^{13}C–^{31}P GHMBC spectrum where ^{31}P would be the high sensitivity nuclide. While in principle a 2D projection of a 3D NMR spectrum could be used to access the ^{13}C–^{31}P correlation information derived from the covariance calculation in the present study, the acquisition of the 3D spectrum to be used as a basis for the 2D projection would be expected to consume considerably more spectrometer time than the acquisition of two high-sensitivity 2D NMR spectra. The covariance ^{13}C–^{31}P spectrum shown in Fig. 5 confirms the assignments of the c-PS. Inspection of the correlations at −2.26 ppm δP corresponding to ST19F PS, shows that the two directly bound ^{13}C ($^{3}J_{HP}$) are easily detected (αRha C1 and βManNAc C4). Two additional peaks are also observed, their ^{13}C chemical shifts corresponding to αRha C3 and C5 ($^{5}J_{HP}$). These assignments are able to be made due to lack of overlap in the ^{13}C dimension. αRha H5 overlaps other peaks in the ^{1}H dimension; thus, standard proton-detected heteronuclear experiments could not have unambiguously identified this peak.

Inspection of the shifts corresponding to the three different phosphodiesters from c-PS shows three different correlations that are observed. For the structural diester β-Glc-P-ribitol (δP 1.24 ppm), the two directly bound resonances ($^{3}J_{HP}$) are easily detected (βGlc C6 and ribitol C5). However, the most intense peak at this ^{31}P chemical shift in the covariance spectrum is at 72.14 ppm δC. This is a region of the spectrum that is severely overlapped in the ^{13}C dimension (Fig. 2). Draing et al. (2006) identified one peak at ~3.77/77.1 ppm that was assigned to ribitol H4. In our sample, this peak resonates at 3.75/72.18; there is no c-PS peak at ~77 ppm δC in our sample. In the ST19F/c-PS mixture, there are two additional peaks at this carbon chemical shift (72.1), the αGlc H3 and βManNAc H3. The αGlc H3 can be excluded based upon the structure of ST19F and βManNAc H3 can be excluded based upon the phosphorus chemical shift. In the proton dimension, this region only has two resonances: the αGlc H6/H6′ methylene and a methine peak at 3.75, presumably from c-PS due to its low intensity compared to the PS peaks. Since, the covariance processing retains multiplicity editing information, it is easily to see that this intense peak at 1.23/72.14 (Fig. 5) must be the ribitol H4 ($^{4}J_{HP}$).

The two pendant phosphodiesters of c-PS have different responses to the covariance processing. The βGalNAc PC (−0.32 ppm δP) shows correlations to its directly bound carbons (PC C1 and βGalNAc C6, $^{3}J_{HP}$). The αGalNAc PC (−0.81 ppm δP) does not show the directly bound carbons. Instead, it has a strong correlation to the PC C2 ($^{4}J_{HP}$). There are unassigned methine correlations which are presumed to be to the ring carbons of βGalNAc and αGalNAc. However, in this situation, these cannot be fully resolved due to overlap in that dimension.

Conclusions

We have demonstrated the use of of ^{1}H–^{31}P HMBC for the assignment of phosphodiesters in polysaccharides. This method is much more sensitive than the "standard" pulse sequence (^{1}H–^{31}P GHSQC). Furthermore, the experiment has also been shown to be "tuneable" for a variety of couplings from $^{3}J_{HP}$ to $^{5}J_{HP}$. The high sensitivity of this experiment allows the complete ^{1}H–^{31}P connectivities of a molecule at the 3% level of the total mass in solution to be unambiguously determined. We have also demonstrated

the first use of covariance processing to calculate a carbon-phosphorus long-range heteronuclear correlation spectrum. The ^{13}C–^{31}P long-range correlation spectrum facilitates the assignments of linkages in the molecule by taking advantage of the greater chemical shift dispersion of ^{13}C versus ^{1}H, allowing the correlations for the minor component of the sample to be detected with significantly greater sensitivity than is possible from even the ^{1}H–^{31}P GHMBC spectrum. Similar sensitivity gains have been obtained by combining low sensitivity experiments such as 1,1-ADEQUATE with a high sensitivity multiplicity-edited GHSQC spectrum (Martin et al. 2011a, b) We are continuing to explore the utilization of covariance NMR methods versus the direct acquisition of, for example ^{31}P-detected ^{13}C–^{31}P GHMBC correlation spectra. The results of these studies will serve as the basis for future reports.

Acknowledgments We would like to thank Kirill Blinov of ACD, Moscow Department and Carlos Cobas of Mestrenova for implementing covariance processing in their software. ERZ would like to thank Dave Detlefsen for the initial idea to use HMBC instead of HSQC and John Limtiaco for discussions of the HMBC sequence and pointing out the use of constant-time HMBC to eliminate twisting in the indirect dimension.

References

Abeygunawardana C, Williams TC, Sumner JS, Hennessey JP (2000) Development and validation of an NMR-based identity assay for bacterial polysaccharides. Anal Biochem 279:226–240

Aubin Y, Jones C, Freedberg DI (2010) Using NMR Spectroscopy to obtain the higher order structure of biopharmaceutical products. Biopharm Int Supplement, 28–34

Bax A, Summers MF (1986) Proton and carbon-13 assignments from sensitivity enhanced detection of heteronuclear multiple-bond connectivity by 2D multiple quantum NMR. J Am Chem Soc 108:2093–2094

Berger S (2010) 2D carbon-heteroatom correlation. In: Morris GA, Emsley JW (eds) Multidimensional NMR methods for the solution state. Wiley, New York, pp 365–372

Blinov KA, Larin N, Williams AJ, Zell M, Martin GE (2006a) Long-range carbon–carbon connectivity via unsymmetrical indirect covariance processing of HSQC and HMBC NMR data. Magn Reson Chem 44:107–109

Blinov KA, Larin N, Williams AJ, Mills K, Martin GE (2006b) Unsymmetrical covariance processing of COSY or TOCSY and HSQC NMR data to obtain the equivalent of HSQC-COSY and HSQC-TOCSY Spectra. J Heterocycl Chem 43:163–166

Catoire LJ (2004) Phosphorus-31 transverse relaxation rate measurements by NMR spectroscopy: insight into conformational exchange along the nucleic acid backbone. J Biomol NMR 28:179–184

Chary KVR, Rastogi VK, Govil G (1993) An Efficient 2D NMR technique helco for heteronuclear [P-31-H-1] long-range correlation. J Magn Reson Ser B 102:81–83

Chen YB, Zhang FL, Snyder D, Gan ZH, Bruschweiler-Li L, Bruschweiler R (2007) Quantitative covariance NMR by regularization. J Biomol NMR 38:73–77

Claridge TDW, Perez-Victoria I (2003) Enhanced C-13 resolution in semi-selective HMBC: a band-selective, constant-time HMBC for complex organic structure elucidation by NMR. Org Biomol Chem 1:3632–3634

Davies DB, Eaton RJ, Baranovsky SF, Veselkov AN (2000) NMR investigation of the complexation of daunomycin with deoxytetranucleotides of different base sequence in aqueous solution. J Biomol Struct Dyn 17:887–901

Draing C, Pfitzenmaier M, Zummo S, Mancuso G, Geyer A, Hartung T, von Aulock S (2006) Comparison of lipoteichoic acid from different serotypes of *Streptococcus pneumoniae*. J Biol Chem 281:33849–33859

Furrer J (2010) A robust, sensitive, and versatile HMBC experiment for rapid structure elucidation by NMR: IMPACT-HMBC. Chem Comm 46:3396–3398

ICH Harmonised Tripartite Guideline. Specifications: test procedures and acceptance criteria for biotechnological/biological products Q6B

Jennings HJ, Rosell KG, Carlo DJ (1980) Structural determination of the capsular polysaccharide of *Streptococcus pneumoniae* type-19 (F-19). Can J Chem 58:1069–1074

John CM, Liu MF, Jarvis GA (2009a) Profiles of structural heterogeneity in native lipooligosaccharides of Neisseria and cytokine induction. J Lipid Res 50:424–438

John CM, Liu MF, Jarvis GA (2009b) Natural phosphoryl and acyl variants of lipid a from *Neisseria meningitidis* strain 89I differentially induce tumor necrosis factor-alpha in human monocytes. J Biol Chem 284:21515–21525

Jones C (1985) Identification of the tetrasaccharide repeating-unit of the *Streptococcus pneumoniae* type-23 polysaccharide by high-field proton NMR-spectroscopy. Carbohydr Res 139:75–83

Kamerling JP (2000) Pneumococcal polysaccharides: a chemical view. In: Tomasz A (ed) *Streptococcus pneumoniae* molecular biology and mechanisms of diseases. Mary Ann Liebert, Larchmont, pp 81–114

Keniry MA (1996) Pulsed field gradient pulse sequence for heteronuclear [P-31-H-1] long range correlation. Magn Reson Chem 34:33–35

Kozminski W, Bednarek E, Bocian W, Sitkowski J, Kozerski L (2003) The new HMQC-based technique for the quantitative determination of heteronuclear coupling constants. Application for the measurement of (3)J(H′(i,) Pi+1) in DNA oligomers. J Magn Reson 160:120–125

Lindon JC, Baker DJ, Farrant RD, Williams JM (1986) H-1, C-13 and P-31 Nmr-spectra and molecular-conformation of myoinositol 1,4,5-trisphosphate. Biochem J 233:275–277

Luy B, Marino JP (2001) J. Am Chem Soc 123:11306–11307

Majumdar A, Shah MH, Bitok JK, Hassis-LeBeau ME, Meyers CLF (2009) Probing phosphorylation by non-mammalian isoprenoid biosynthetic enzymes using H-1-P-31-P-31 correlation NMR spectroscopy. Mol Biosyst 5:935–944

Majumdar A, Sun Y, Shah M, Meyers CLF (2010) Versatile H-1-P-31-P-31 COSY 2D NMR techniques for the characterization of polyphosphorylated small molecules. J Org Chem 75:3214–3223

Malon M, Koshino H (2007) H(C)P and H(P)C triple-resonance experiments at natural abundance employing long-range couplings. Magn Reson Chem 45:770–776

Marek R, Lyčka R, Lyčka A (2002) ^{15}N NMR spectroscopy in structural analysis. Curr Org Chem 6:35–66

Marek R, Lyčka A, Kolehmainen E, Sieväen E, Toušek J (2007) 15N NMR spectroscopy in structural analysis: an update (2001–2005). Curr Org Chem 11:1154–1205

Martin GE (2002a) Qualitative and quantitative exploitation of heteronuclear coupling constants. In: Webb GA (ed) Annual report on NMR spectroscopy, vol 46. Academic Press, New York, pp 37–101

Martin GE (2002b) Cryogenic NMR probes. In: Grant DM, Harris RK (eds) Encyclopedia of nuclear magnetic resonance, vol 9 supplement. Wiley, New York, pp 33–35

Martin GE (2005) Small-volume and high-sensitivity NMR probes. In: Webb GA (ed) Annual report on NMR spectroscopy, vol 56. Elsevier, Amsterdam, pp 2–96

Martin GE, Hadden CE (2000) Techniques for long-range 1H–15N heteronuclear shift correlation at natural abundance and applications to structural problems. J Nat Prod 63:543–585

Martin GE, Williams AJ (2005) Long-range ^{1}H–^{15}N heteronuclear shift correlations. In: Webb GA (ed) Annual report on NMR spectroscopy, vol 55. Elsevier, Amsterdam, pp 2–119

Martin GE, Williams AJ (2010) Utilizing long-range ^{1}H–^{15}N 2D NMR spectroscopy for chemical structure elucidation and confirmation: encyclopedia of NMR spectroscopy, Wiley, New York (in press)

Martin GE, Hilton BD, Blinov KA, Williams AJ (2007a) 13C–15N correlation via unsymmetrical indirect covariance NMR: application to vinblastine. J Nat Prod 70:1966–1970

Martin GE, Irish PA, Hilton BD, Blinov KA, Williams AJ (2007b) Utilizing unsymmetrical indirect covariance processing to define 15 N–13C connectivity networks. Magn Reson Chem 45:624–627

Martin GE, Hilton BD, Blinov KA (2011a) HSQC-ADEQUATE: a new paradigm for establishing molecular skeletons. Magn Reson Chem 49:248–252

Martin GE, Hilton BD, Willcott MR III, Blinov KA (2011b) HSQC-ADEQUATE: a further Investigation of data requirements. Magn Reson Chem 49:350–358

Pujar NS, Huang NF, Daniels CL, Dieter L, Gayton MG, Lee AL (2004) Base hydrolysis of phosphodiester bonds in pneumococcal polysaccharides. Biopolymer 75:71–84

Richards JC, Perry MB (1988) Structure of the specific capsular polysaccharide of *Streptococcus pneumoniaetype*-23F (American Type-23). Biochem Cell Biol 66:758–771

Roy A, Roy N (1984) Structure of the capsular polysaccharide from *Streptococcus pneumoniae* type-23. Carbohydr Res 126:271–277

Sakamoto Y, Kondo K, Onozato M, Aoyama T (2006) Conformational analysis of 2-(diphenylphosphanyl)-N, N-dimethyl-1-benz amide and 2-(diphenylphosphanyl)-phenyl-pyrrolidin-1-YL-methanone by NMR spectroscopy. Polycycl Aromat Compd 26:59–68

Schoefberger W, Schlagnitweit J, Muller N (2011) Ann. Rep NMR Spectrosc 72:1–60

Sims LD, Soltero LR, Martin GE (1989) Carbon-phosphorous heteronuclear shift correlation via multiple quantum coherence. Magn Reson Chem 27:599–602

Snyder DA, Brüschweiler R (2009) Generalized indirect covariance NMR Formalism for the establishment of multidimensional spin correlations. J Chem Phys A 113:12898–12902

Snyder DA, Brüschweiler R (2010) Multi-dimensional correlation spectroscopy by covariance NMR. In: Morris GA, Emsley JW (eds) Multidimesional NMR methods in the solution state. Wiley, New York, pp 97–105

Veselkov AN, Eaton RJ, Pakhomov VI, Djimant LN, Davies DB (2001) Structural and thermodynamic analysis of daunomycin binding with desoxyhexanucleotides with different base sequences by NMR spectroscopy. J Struct Chem 42:193–206

Watson JD, Crick FHC (1953) A structure for deoxyribose nucleic acid. Nature 171:737–738

Williamson MP, Griffin CE (1968) Three- and four-bond 31P–1H coupling constants and geminal proton nonequivalence in ethyl esters of phosphorus acids. J Phys Chem 72:4043–4047

Willker W, Leibfritz D (1995) Determination of heteronuclear long-range H, X coupling-constants from gradient-selected Hmbc spectra. Magn Reson Chem 33:632–638

Xu QW, Abeygunawardana C, Ng AS, Sturgess AW, Harmon BJ, Hennessey JP (2005) Characterization and quantification of C-polysaccharide in Streptococcus pneumoniae capsular polysaccharide preparations. Anal Biochem 336:262–272

Zartler ER, Porambo RJ, Anderson CL, Chen LH, Yu JG, Nahm MH (2009) Structure of the capsular polysaccharide of pneumococcal serotype 11A reveals a novel acetylglycerol that is the structural basis for 11A subtypes. J Biol Chem 284:7318–7329